Harper et al., 2018, Subtropical sea-surface warming and increased salinity during Eocene Thermal Maximum 2: Geology, https://doi.org/10.1130/G39658.1.

SUPPLEMENTAL INFORMATION

LOSCAR SIMULATION OF ETM-2

We apply the LOSCAR (Long-term Ocean-atmosphere-Sediment CArbon cycle Reservoir Model v2.0.4; Zeebe, 2012) climate/carbon-cycle model to simulate the ETM-2 carbon emission scenario given observations of CCD, planktic $\delta^{13}C$ and ΔSST (see Fig. DR2), with the goal of generating ΔpH estimates across the event so that pH-adjustments may be applied to planktic $\delta^{18}O$ and Mg/Ca. This model has been used extensively in previous research to simulate PETM and modern emission scenarios (Zachos et al., 2008; Zeebe et al., 2009; Sluijs et al., 2012; Zeebe, 2013; Zeebe and Zachos 2013; Penman et al., 2014; Zeebe et al., 2016). We apply the same boundary conditions (i.e., early Eocene ocean geometry and climate response functions based on early Eocene climate sensitivity) used in recent PETM simulations (Zeebe et al., 2016). We then simulate the carbon emission scenario by releasing 1,300 Pg C over 25 kyr, at time = 0 kyr (consistent with the astronomically-paced onset described in Lourens et al. (2005)), using an intermediate $\delta^{13}C$ of −40‰, with the aim of matching simulations to observations of the magnitude of the CIE and CCD changes (Fig. DR2). The ETM-2 simulation indicates a pH decrease of ~0.05. The temperature anomaly produced by this simulation falls within the range of pH-adjusted and non-adjusted Mg/Ca-based temperatures (Fig. DR3).

ANALYTICAL CHEMISTRY

Foraminifera (25 individuals) were crushed, homogenized, and split into two samples, one for trace elements and one for stable isotopes ($\delta^{13}C$/$\delta^{18}O$). Trace element samples were cleaned following the oxidative reductive protocol of Barker et al. (2003), dissolved in 0.075N HNO_3 and analyzed via ICP-MS on a Thermo Element XR following the methodology of Brown et al. (2011). The long-term reproducibility of consistency standard measurements indicates inter-run precision for Mg/Ca is <3% (2 s.d.).

The sample portion used for stable isotope analysis was not cleaned following oxidation/reduction protocol. These samples were analyzed on a Thermo MAT 253 IR-MS coupled to a Kiel IV carbonate device. Based on replicate measurements of consistency standards, inter-run precision for $\delta^{13}C$ and $\delta^{18}O$ is <0.1% (2 RSD) and <0.16% (2 RSD), respectively. The bulk %$CaCO_3$ ETM-2 record for Site 1209 was generated using a UIC Carbon Coulometer Analyzer.

ΔSST AND ΔSSS COMPUTATIONS

Planktic Mg/Ca is pH-adjusted using the LOSCAR-simulated ΔpH for ETM-2 following the logistic pH-adjustment from Evans et al. (2016):

$$\mathrm{Mg/Ca} = \frac{0.66}{1+\exp\left(6.9*(\mathrm{pH}-8.0)\right)} + 0.76. \quad (1)$$

Additionally, because Evans et al. (2016) could not rule out a linear fit to their data, we also include the linear pH-adjustment in our SST and SSS anomaly envelopes:

$$\mathrm{Mg/Ca} = -0.70 * \mathrm{pH} + 6.7. \quad (2)$$

These pH-adjustments shift temperatures by <0.1°C due to the small pH decrease (~−0.05 pH units) we simulate for ETM-2. Furthermore, when larger magnitude boron-based ΔpH (~−0.11 pH units) is applied, the added effect on ΔSST is less than −0.1°C, and less than −0.2 ppt for ΔSSS (Fig. DR3). SST anomalies are generated using the pH-adjusted planktic Mg/Ca following Zachos et al. (2003):

$$\Delta T = \frac{1}{A}\ln\left[\left(\frac{C}{100}\right)+1\right]. \quad (3)$$

Where 'C' is the percent change in Mg/Ca relative to baseline and 'A' is the exponential constant in the Mg/Ca-temperature calibration (i.e., Mg/Ca-temperature sensitivity for a species of foraminifera). Here we apply a range of 'A' values derived using culture calibration measurements of the modern species *G. ruber* in which $Mg/Ca_{seawater}$ was varied, following Evans et al. (2016). The best regression fits through the culture calibration data indicate a decrease in sensitivity (i.e., lower 'A' value) with lower $Mg/Ca_{seawater}$. Given the possible range of $Mg/Ca_{seawater}$ in the early Eocene, we apply a range in 'A' values of 0.05 to 0.09 to generate SST anomaly envelopes. This method incorporates errors due to the potential uncertainty in $Mg/Ca_{seawater}$ for the early Eocene, however, it is still limited due to the fact that sensitivities are based on culture calibration of a single modern planktic foraminifera species. Anomaly envelopes do not incorporate any changes in $Mg/Ca_{seawater}$ across the hyperthermal, which is appropriate given the residence times of Mg and Ca in seawater (~13 Ma and ~1 Ma, respectively; Broecker and Peng, 1982) and the time interval of the anomaly envelope (~200 kyr).

To generate SSS anomaly envelopes, we assume any difference in pH-adjusted $\delta^{18}O$-based ΔSST compared to pH-adjusted Mg/Ca-based ΔSST is due to the effect of local surface salinity changes on $\delta^{18}O$. Mg/Ca-based ΔSSTs are converted into expected $\delta^{18}O$ temperature anomalies following the relationship of 0.213‰/°C from Zachos et al. (2003). We then subtract the pH-adjusted (−2.51‰ per pH unit following Zeebe, 1999) observed $\delta^{18}O$ anomaly from a theoretical temperature-based $\delta^{18}O$ record generated using the Mg/Ca-based temperature change. This produces a residual $\delta^{18}O$ anomaly. This residual value represents the surface salinity signal in planktic $\delta^{18}O$. SSS anomaly envelopes incorporate both the range in the Mg/Ca-temperature calibration constants and the possible range of the $\Delta\delta^{18}O$seawater / ΔSSS relationship (0.25-0.50‰/salinity unit) from Zachos et al. (2003).

REFERENCES CITED

Barker, S., Greaves, M., and Elderfield, H., 2003, A study of cleaning procedures used for foraminiferal Mg/Ca paleothermometry: Geochemistry Geophysics Geosystems, v. 4, no. 9.

Broecker, W. S., and Peng, T. H., 1982, Tracers in the Sea, p. 125-159.

Brown, R. E., Anderson, L. D., Thomas, E., and Zachos, J. C., 2011, A core-top calibration of B/Ca in the benthic foraminifers *Nuttallides umbonifera* and *Oridorsalis umbonatus*: A proxy for Cenozoic bottom water carbonate saturation: Earth and Planetary Science Letters, v. 310, no. 3, p. 360-368.

Evans, D., Wade, B. S., Henehan, M., Erez, J., and Müller, W., 2016, Revisiting carbonate chemistry controls on planktic foraminifera Mg/Ca: implications for sea surface temperature and hydrology shifts over the Paleocene–Eocene Thermal Maximum and Eocene–Oligocene Transition: Climate of the Past, v. 11, p. 3143-3185.

Penman, D. E., Hönisch, B., Zeebe, R. E., Thomas, E. and Zachos, J. C., 2014, Rapid and sustained surface ocean acidification during the Paleocene-Eocene Thermal Maximum: Paleoceanography, v. 29, p. 357–369.

Sluijs, A., Zachos, J. C., and Zeebe, R. E., 2012, Constraints on hyperthermals: Nature Geoscience, v. 5, no. 4, p. 231-231.

Zachos, J. C., Wara, M. W., Bohaty, S. M., Delaney, M. L., Rose-Petrizzo, M., Brill, A., Bralower, T. J. and Premoli-Silva, I., 2003, A transient rise in tropical sea surface temperature during the Paleocene-Eocene Thermal Maximum: Science, v. 302, p. 1551–1554.

Zachos, J. C., Dickens, G. R. and Zeebe, R. E., 2008, An early Cenozoic perspective on greenhouse warming and carbon-cycle dynamics: Nature, v. 451, p. 279–283.

Zeebe, Richard E., 1999, An explanation of the effect of seawater carbonate concentration on foraminiferal oxygen isotopes: Geochimica et Cosmochimica Acta, v. 63, no. 13, p. 2001-2007.

Zeebe, R. E., Zachos, J. C., and Dickens, G. R., 2009, Carbon dioxide forcing alone insufficient to explain Palaeocene–Eocene Thermal Maximum warming: Nature Geoscience*,* v.2, no. 8, p. 576-580.

Zeebe, R. E., 2012, LOSCAR: Long-term Ocean-atmosphere-Sediment CArbon cycle Reservoir Model v2.0.4: Geoscientific Model Development, v. 5, p. 149–166.

Zeebe, R. E., 2013, What caused the long duration of the Paleocene-Eocene Thermal Maximum?: Paleoceanography, v. 28, no. 3, p. 440-452.

Zeebe, R. E. and Zachos, J. C., 2013, Long-term legacy of massive carbon input to the Earth system: Anthropocene vs. Eocene: Royal Soc. London Phil. Trans. A., v. 371, no. 2001.

Zeebe, R. E., Ridgwell, A., and Zachos, J. C., 2016, Anthropogenic carbon release rate unprecedented during the past 66 million years: Nature Geoscience, v. 9, no. 4, p. 325-329.

FIGURE CAPTIONS

Figure DR1. Bulk carbonate and carbonate nodule $\delta^{13}C$ from pelagic ocean sites (ODP Sites 1265 and 1209; Stap et al., 2009 and Gibbs et al., 2012) and terrestrial Big Horn Basin Site (Abels et al., 2012) illustrate that the perturbation to carbon cycle during ETM-2 was global. Site 1265 ages are based on the bulk carbonate Site 1263 age model of Lauretano et al. (2016).

Figure DR2. LOSCAR carbon emission scenario for ETM-2: 1,300 Pg of carbon is released to atmosphere at time=0 kyr with $\delta^{13}C$=-40‰. pH simulations for the emission scenario are used to pH-adjust planktic Mg/Ca and $\delta^{18}O$.

Figure DR3. Sensitivity test showing the potential influence of pH adjustment on our SST and SSS records at Sites 1209 and 1265 using 3 different pH change scenarios. The black line represents constant pH. The red line represents a pH change of -0.05 pH units derived from LOSCAR simulations and used in this study. We show both the linear and logistic pH adjustments of Evans et al. (2016). Intermediate values for the Mg/Ca temperature calibration sensitivity ('A' value of 0.075) and intermediate $\delta^{18}O$-salinity sensitivity (0.33‰ per salinity unit) are applied instead of the ranges used previously to clearly display the change in the ΔSST and ΔSSS records for each ΔpH scenario.

Figure DR4. ΔSST and ΔSSS for the PETM at ODP Site 1209 using foraminiferal data (mixed-layer dweller *Acarinina soldadoensis*) from Zachos et al. (2003), which is pH-adjusted using Pacific surface ΔpH data from LOSCAR PETM simulations (Zeebe et al., 2009). SST envelopes are generated similarly to ETM-2 envelopes (Fig. 2) using a range of Mg/Ca-temperature sensitivities ('A' values from 0.05 to 0.09) and include both linear and logistic pH-adjustments from Evans et al. (2016). Note that the larger range in both SST and SSS envelopes shown here, compared with Zachos et al. (2003), is a function of the larger range of Mg/Ca temperature sensitivities given the recommendations of Evans et al. (2016) (see main text). The range in ΔSSS incorporates a range of $\delta^{18}O$-salinity sensitivities (the same range as the ΔSSS envelopes displayed in Fig. 2; 0.25-0.5‰ per salinity unit).

Fig. DR1

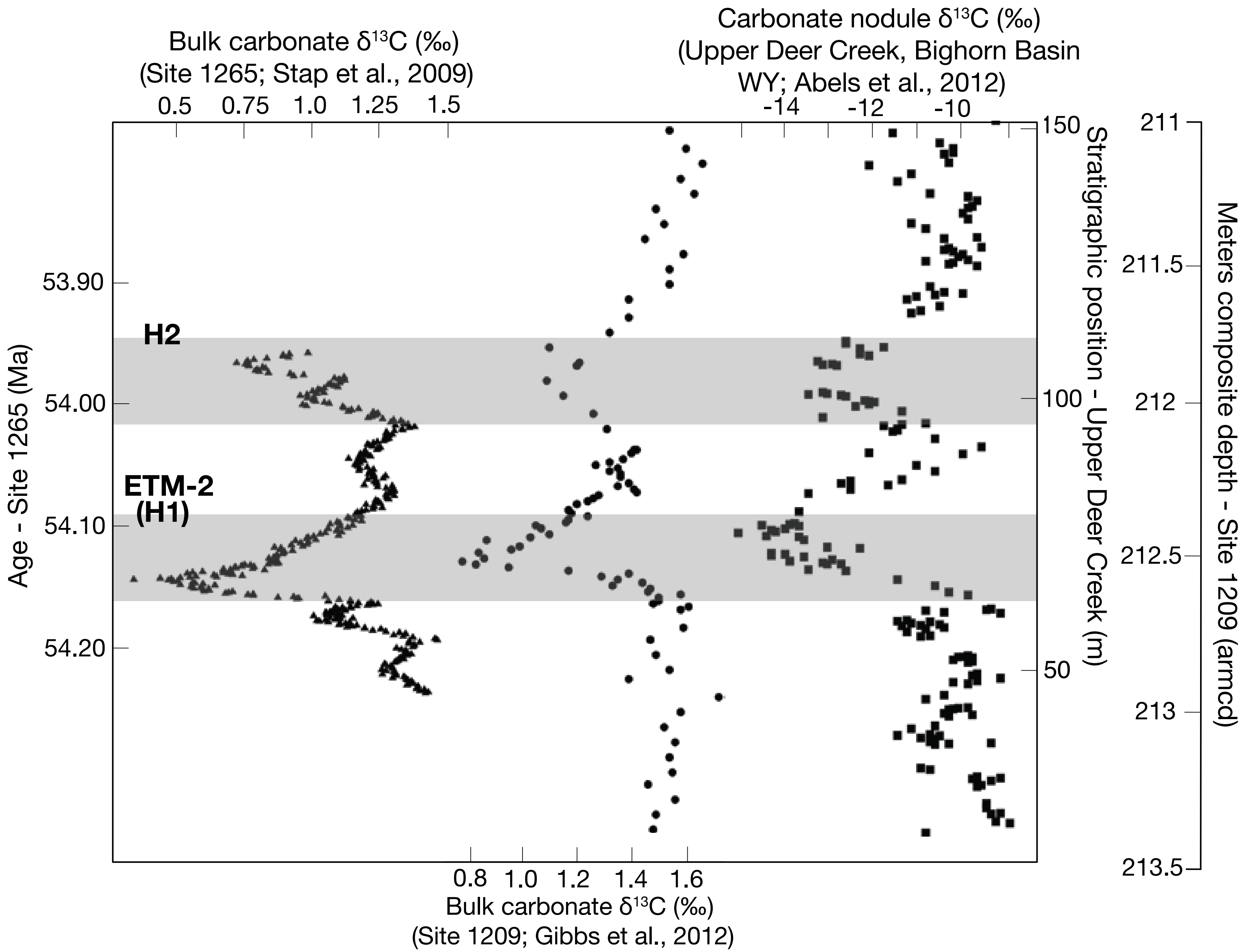

Bulk carbonate δ13C (‰)
(Site 1265; Stap et al., 2009)
0.5
0.75
1.0
1.25
1.5
Carbonate nodule δ13C (‰)
(Upper Deer Creek, Bighorn Basin
WY; Abels et al., 2012)
-14
-12
-10
150
100
50
Stratigraphic position - Upper Deer Creek (m)
211
211.5
212
212.5
213
213.5
Meters composite depth - Site 1209 (armcd)
53.90
54.00
54.10
54.20
Age - Site 1265 (Ma)
H2
ETM-2
(H1)
0.8
1.0
1.2
1.4
1.6
Bulk carbonate δ13C (‰)
(Site 1209; Gibbs et al., 2012)

Fig. DR2

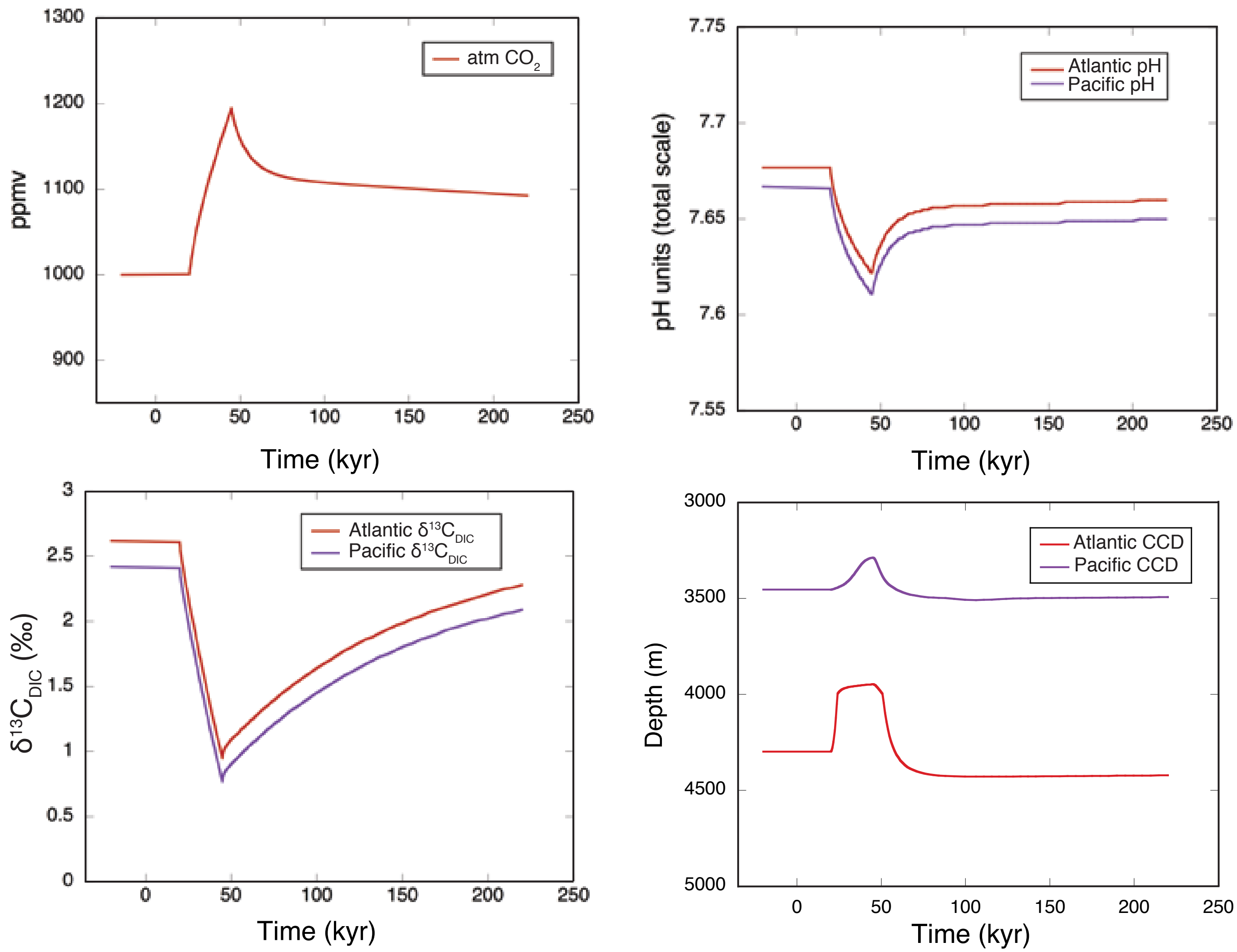

atm CO_2
ppmv
1300
1200
1100
1000
900
0
50
100
150
200
250
Time (kyr)
Atlantic pH
Pacific pH
pH units (total scale)
7.75
7.7
7.65
7.6
7.55
Time (kyr)
Atlantic $\delta^{13}C_{DIC}$
Pacific $\delta^{13}C_{DIC}$
$\delta^{13}C_{DIC}$ (‰)
3
2.5
2
1.5
1
0.5
0
Time (kyr)
Atlantic CCD
Pacific CCD
Depth (m)
3000
3500
4000
4500
5000
Time (kyr)

Fig. DR3

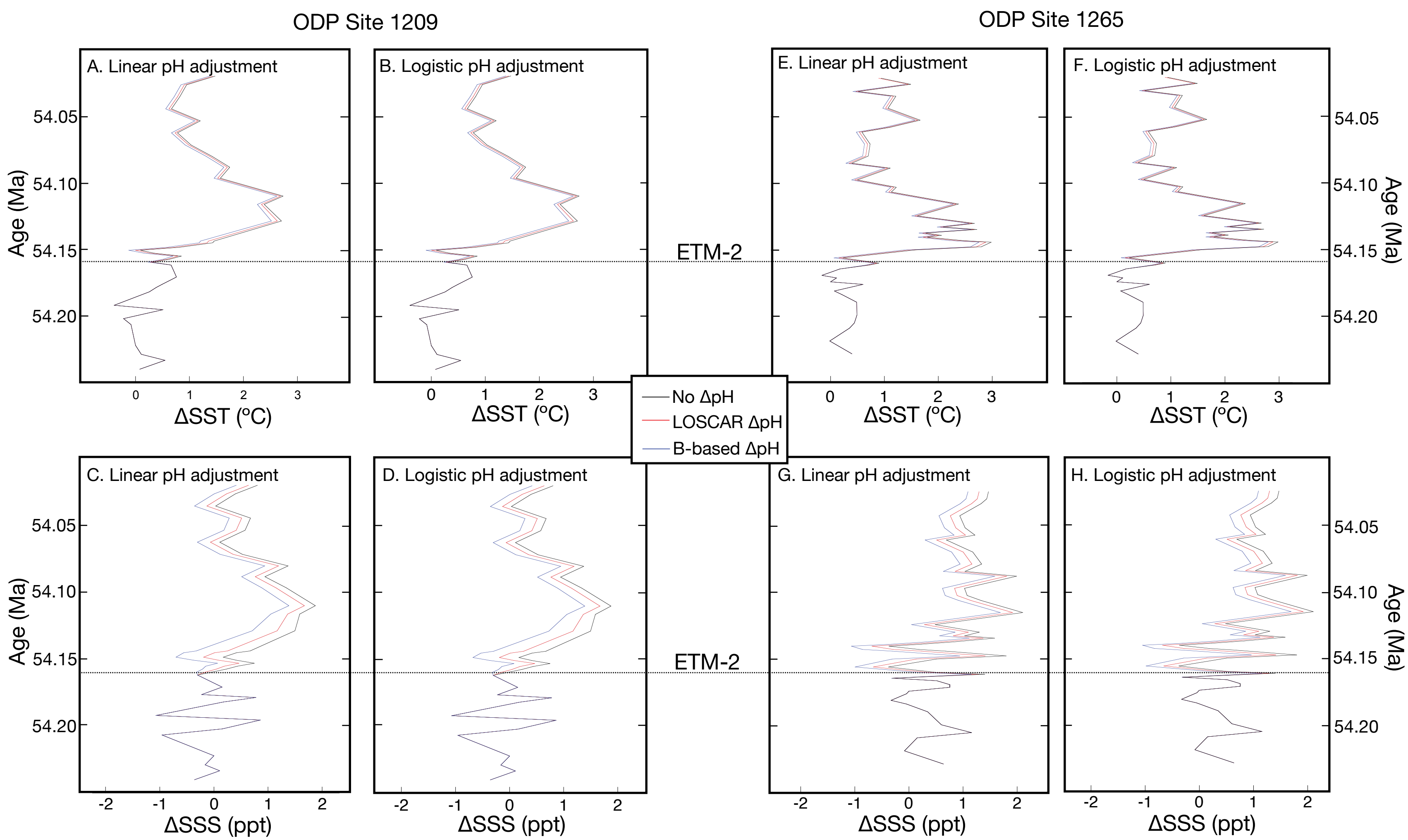

ODP Site 1209
ODP Site 1265
A. Linear pH adjustment
B. Logistic pH adjustment
E. Linear pH adjustment
F. Logistic pH adjustment
C. Linear pH adjustment
D. Logistic pH adjustment
G. Linear pH adjustment
H. Logistic pH adjustment
Age (Ma)
54.05
54.10
54.15
54.20
ETM-2
ΔSST (ºC)
ΔSSS (ppt)
No ΔpH
LOSCAR ΔpH
B-based ΔpH

Fig. DR4

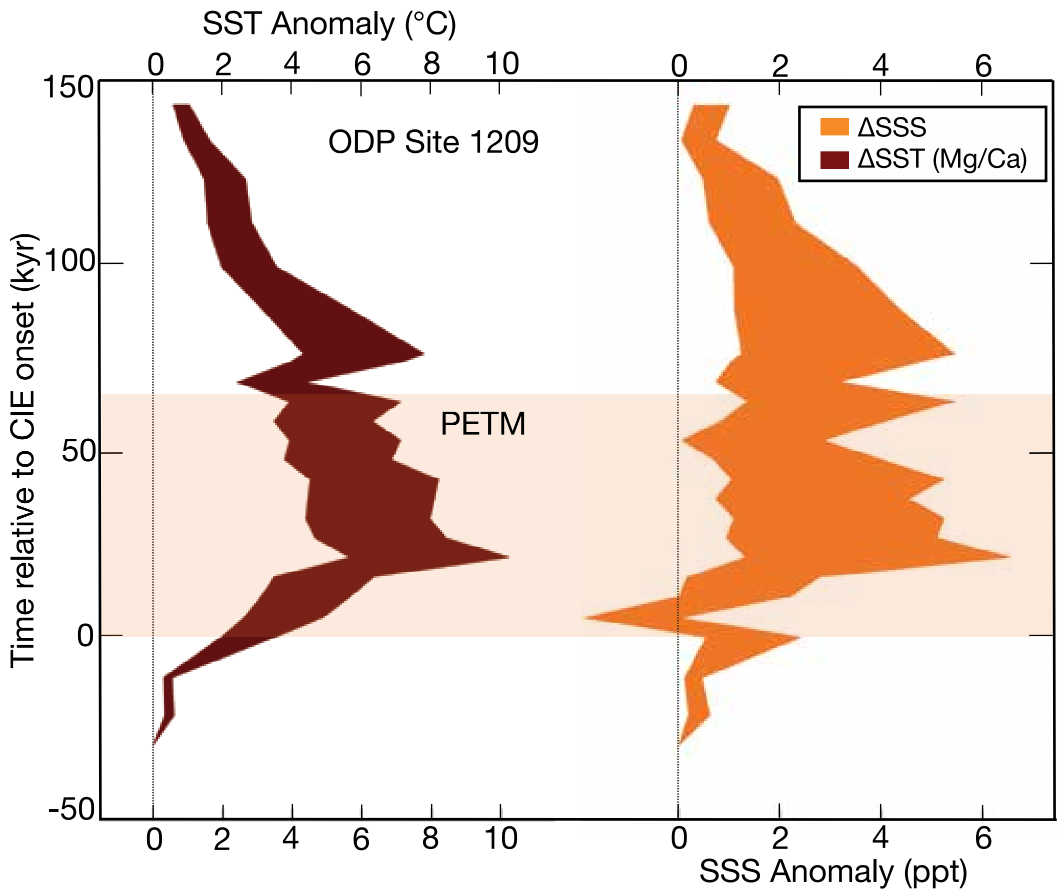

SST Anomaly (°C)
0 2 4 6 8 10
0 2 4 6
ODP Site 1209
ΔSSS
ΔSST (Mg/Ca)
PETM
Time relative to CIE onset (kyr)
150
100
50
0
-50
0 2 4 6 8 10
0 2 4 6
SSS Anomaly (ppt)